Cyclical Dissipation in Cryptographic Assets: Wavelet Spectral Decomposition and Variance Compression Across Bitcoin Market Eras

Peter Mancini
krahang@pm.me

August 22, 2026

Abstract

For over a decade, Bitcoin's price trajectory and market narrative have been defined by the four-year programmatic block-reward halving schedule. Early empirical models posited that periodic supply-side shocks serve as the primary governing mechanism for macro bull-market expansions and cyclical peaks. In this paper, we conduct a longitudinal spectral and distributional analysis of Bitcoin daily reference rates from July 2010 to May 2026 across four distinct structural market eras. By detrending price series against a secular log-log power-law baseline, we evaluate the persistence of cyclical harmonics using Lomb-Scargle periodograms and Morlet Continuous Wavelet Transforms (CWT). We demonstrate that the spectral power concentrated at the theoretical $\sim$ 1,460-day (4-year) halving frequency has decayed precipitously ($\mathcal{P}_W > 900 \rightarrow \mathcal{P}_W \leq 200$), indicating cyclical dissipation. Concurrently, non-parametric quantile analysis demonstrates monotonic variance compression across eras: the 5th/95th percentile daily return corridor has halved ($[-7.61\%, +8.84\%] \rightarrow [-3.86\%, +4.13\%]$), annualized tail volatility has declined by 66.5%, and residual dispersion has dropped by 73.1%. Our findings suggest that institutional market integration—culminating in regulated spot exchange-traded funds—has decoupled Bitcoin from its mining-driven four-year rhythm, transitioning the asset into a continuous macroeconomic reserve asset governed by global liquidity cycles.

1 Introduction

1.1 The Four-Year Halving Paradigm

Since the mining of the Genesis Block in 2009, the Bitcoin network's programmatic disinflationary monetary policy has served as the bedrock for cyclical market expectations. Every 210,000 blocks ($\approx$ 1,460 days), the protocol-mandated subsidy awarded to miners halves, reducing the daily nominal issuance of newly minted tokens. In the asset's first three epochs (2012, 2016, and 2020), each halving event was followed within 12 to 18 months by an explosive macro expansion, establishing a widespread consensus that supply-side flow deficits are the primary causal driver of multi-year price discovery.

This mechanical perspective spawned popular econometric frameworks—most notably stock-to-flow and unconstrained exponential step models—which assumed that periodic supply contractions would perpetually induce recursive, high-amplitude speculative cycles.

1.2 Institutional Maturation and Economic Friction

While the halving supply shock hypothesis proved explanatory during Bitcoin's nascent, illiquid phases, fundamental macroeconomic and market microstructure forces impose two critical constraints as the asset scales:

1. **Diminishing Marginal Flow Shock:** When daily network issuance decreased from 50 BTC to 25 BTC per block in 2012, the nominal reduction represented a massive fraction of available floating supply and daily exchange volume. At current subsidy levels (3.125 BTC per block), the daily newly issued supply (≈ 450 BTC) constitutes a negligible fraction of global daily spot and derivative turnover.

2. **Institutional Ingress and Capital Scale:** The integration of cash-settled CME futures (2017), corporate balance sheet allocations (2020), and regulated spot exchange-traded funds (2024) fundamentally transformed the participant base. Bitcoin transitioned from a retail-dominated, fragmented order book environment into deep institutional clearinghouses integrated with sovereign macro asset allocators.

1.3 Research Contributions and Thesis

In this paper, we challenge the assumption that Bitcoin remains bound to a perpetual four-year periodic clock. We provide a rigorous empirical framework to investigate the decay of cyclical harmonics and the structural compression of return distributions.

Our primary contributions are threefold:

- **Continuous Time-Frequency Decomposition:** We apply Morlet Continuous Wavelet Transforms (CWT) and Lomb-Scargle periodograms to detrended secular power-law residuals, tracking the exact temporal dissipation of the 1,460-day harmonic from early dominance to near-baseline noise.

- **Regime-Segmented Variance Quantification:** We measure the parametric and non-parametric compression of return distributions across four distinct market eras, showing a structural halving of daily tail risk and a collapse in annualized volatility.

- **The Institutional Decoupling Hypothesis:** We demonstrate that cyclical expectations anchored strictly to the halving calendar suffer from specification error; Bitcoin's contemporary dynamics are primarily driven by macro-liquidity conditions, interest rate cycles, and institutional portfolio rebalancing.

2 Data and Empirical Pre-processing

2.1 Reference Rate Ingestion and Harmonization

The empirical analysis utilizes daily closing reference rates for Bitcoin (BTC) sourced from CoinMetrics. To ensure temporal consistency across global exchanges and circumvent boundary discontinuities associated with localized trading sessions, each daily observation P_t is strictly standardized to the 00:00:00 UTC median volume-weighted reference rate:

$$P_t \equiv P(\tau_t), \quad \tau_t = t - t_0 \in \mathbb{N}^+, \tag{1}$$

where t_0 denotes the Bitcoin Genesis Block timestamp (2009-01-03 18:15:05 UTC), and τ_t represents the elapsed calendar time in days since inception. The sample spans from July 18, 2010 to May 23, 2026, comprising $N = 5{,}789$ continuous daily observations.

We define the natural logarithmic price y_t and the continuously compounded daily log return r_t as:

$$y_t = \ln(P_t), \tag{2}$$

$$r_t = y_t - y_{t-1} = \ln\left(\frac{P_t}{P_{t-1}}\right). \tag{3}$$

2.2 Deterministic Power-Law Baselining and Residual Isolation

Because Bitcoin exhibits scale-invariant exponential growth across multiple orders of magnitude, standard linear detrending or high-order polynomial fits introduce substantial overfitting and look-ahead distortion. We employ a secular log-log power-law baseline grounded in scale-free network expansion:

$$\ln(P_t) = \alpha + \beta \ln(\tau_t) + \varepsilon_t, \tag{4}$$

where $\alpha \in \mathbb{R}$ represents the network scale intercept at $\tau_t = 1$, $\beta \in \mathbb{R}^+$ denotes the scale-invariance elasticity parameter, and ε_t is the zero-mean cyclical residual error. Ordinary least squares (OLS) estimation yields:

$$\hat{\beta} = 5.6738, \quad \hat{\alpha} = -37.8925 \quad (R^2 \approx 0.924). \tag{5}$$

The detrended residual series $\hat{\varepsilon}_t \equiv y_t - (\hat{\alpha} + \hat{\beta} \ln \tau_t)$ serves as our primary stationary oscillator for subsequent spectral decomposition.

2.3 Structural Market Milestones

Rather than imposing strictly endogenous or arbitrary sample splits, the longitudinal data is partitioned into four non-overlapping macroeconomic and structural market regimes:

1. **Era 1: Early Spot / Peer-to-Peer (2010-07-18 to 2017-12-17):** Characterized by retail-dominated spot exchange order books prior to formal institutional derivatives.

2. **Era 2: Derivatives and Offshore Margin (2017-12-18 to 2020-10-01):** Initiated by the listing of CME Bitcoin Futures and the maturation of perpetual swaps.

3. **Era 3: Corporate Treasury and Macro Ingress (2020-10-02 to 2024-01-10):** Defined by institutional balance sheet adoption (e.g., MicroStrategy) and sovereign legal tender integration.

4. **Era 4: Spot ETF and Regulated Custody (2024-01-11 to Present):** Initiated by the SEC approval of spot exchange-traded funds, providing direct institutional capital pipelines.

3 Spectral Decomposition and Time-Frequency Estimation

3.1 Stationarity and Non-Parametric Harmonic Estimation

Financial return series typically exhibit non-stationary drift, heavy tails, and volatility clustering. By detrending the logarithm of the daily reference rate against the deterministic log-log power-law baseline defined in Equation (4), we obtain a zero-mean cyclical oscillator:

$$\hat{\varepsilon}_t = \ln(P_t) - \left(\hat{\alpha} + \hat{\beta} \ln \tau_t\right). \tag{6}$$

To evaluate whether this residual oscillator contains statistically significant periodic components—specifically testing the hypothesis of a persistent 1,460-day halving cycle—we employ non-parametric frequency domain techniques. Standard Fast Fourier Transforms (FFT) assume strict stationarity and evenly spaced continuous sampling over infinite horizons, which can introduce spectral leakage and edge distortion in finite economic time series.

3.2 Normalized Lomb-Scargle Periodogram

We implement the generalized Lomb-Scargle periodogram [1,2], which fits sinusoidal basis functions via least squares across specified test frequencies. For an arbitrary angular frequency $\omega = 2\pi/T$ (where T represents the harmonic period in days), the spectral power density $P_{LS}(\omega)$ on the detrended series $\{\hat{\varepsilon}_j\}_{j=1}^N$ sampled at times $\{t_j\}_{j=1}^N$ is defined as:

$$P_{LS}(\omega) = \frac{1}{2\sigma^2}\left[\frac{\left(\sum_{j=1}^N(\hat{\varepsilon}_j - \bar{\varepsilon})\cos\omega(t_j-\theta)\right)^2}{\sum_{j=1}^N \cos^2\omega(t_j-\theta)} + \frac{\left(\sum_{j=1}^N(\hat{\varepsilon}_j - \bar{\varepsilon})\sin\omega(t_j-\theta)\right)^2}{\sum_{j=1}^N \sin^2\omega(t_j-\theta)}\right], \tag{7}$$

where $\bar{\varepsilon}$ and σ^2 denote the empirical sample mean and variance:

$$\bar{\varepsilon} = \frac{1}{N}\sum_{j=1}^N \hat{\varepsilon}_j, \quad \sigma^2 = \frac{1}{N-1}\sum_{j=1}^N(\hat{\varepsilon}_j - \bar{\varepsilon})^2. \tag{8}$$

The frequency-dependent phase parameter $\theta(\omega)$ provides time-translation invariance and satisfies:

$$\tan(2\omega\theta) = \frac{\sum_{j=1}^N \sin(2\omega t_j)}{\sum_{j=1}^N \cos(2\omega t_j)}. \tag{9}$$

We evaluate the normalized periodogram over a broad period band $T \in [30, 2000]$ days across both the aggregate sample and within partitioned structural market eras.

3.3 Continuous Wavelet Transform (CWT) and Morlet Scalograms

While the Lomb-Scargle periodogram quantifies global spectral energy across an entire epoch, it integrates over the time domain, obscuring the precise temporal evolution and dissipation of cyclical signals. To capture time-localized frequency shifts, we apply the Continuous Wavelet Transform (CWT) [3].

The continuous wavelet transform of a continuous signal $x(t)$ with respect to an analytic mother wavelet $\psi(t)$ is defined as:

$$W_x(s,\eta) = \int_{-\infty}^{+\infty} x(t)\,\frac{1}{\sqrt{s}}\psi^*\left(\frac{t-\eta}{s}\right)dt, \tag{10}$$

where $s > 0$ represents the dilation scale parameter, $\eta \in \mathbb{R}$ is the temporal translation parameter, and $*$ denotes the complex conjugate.

We utilize the complex Morlet wavelet, consisting of a plane wave modulated by a Gaussian envelope:

$$\psi(t) = \pi^{-1/4}e^{i\omega_0 t}e^{-t^2/2}. \tag{11}$$

We set the non-dimensional central frequency parameter to $\omega_0 = 6$, which provides optimal balance between temporal and frequency localization while satisfying the wavelet admissibility condition ($e^{-\omega_0^2/2} \approx 0$).

3.4 Scale-to-Period Mapping and Power Distribution

To translate non-dimensional wavelet scale s into physical calendar periods T_s, we apply the exact Fourier-equivalent wavelength relation for the Morlet wavelet:

$$T_s = \frac{4\pi s}{\omega_0 + \sqrt{2+\omega_0^2}} \approx \frac{4\pi s}{6+\sqrt{38}} \approx 1.03304\,s. \tag{12}$$

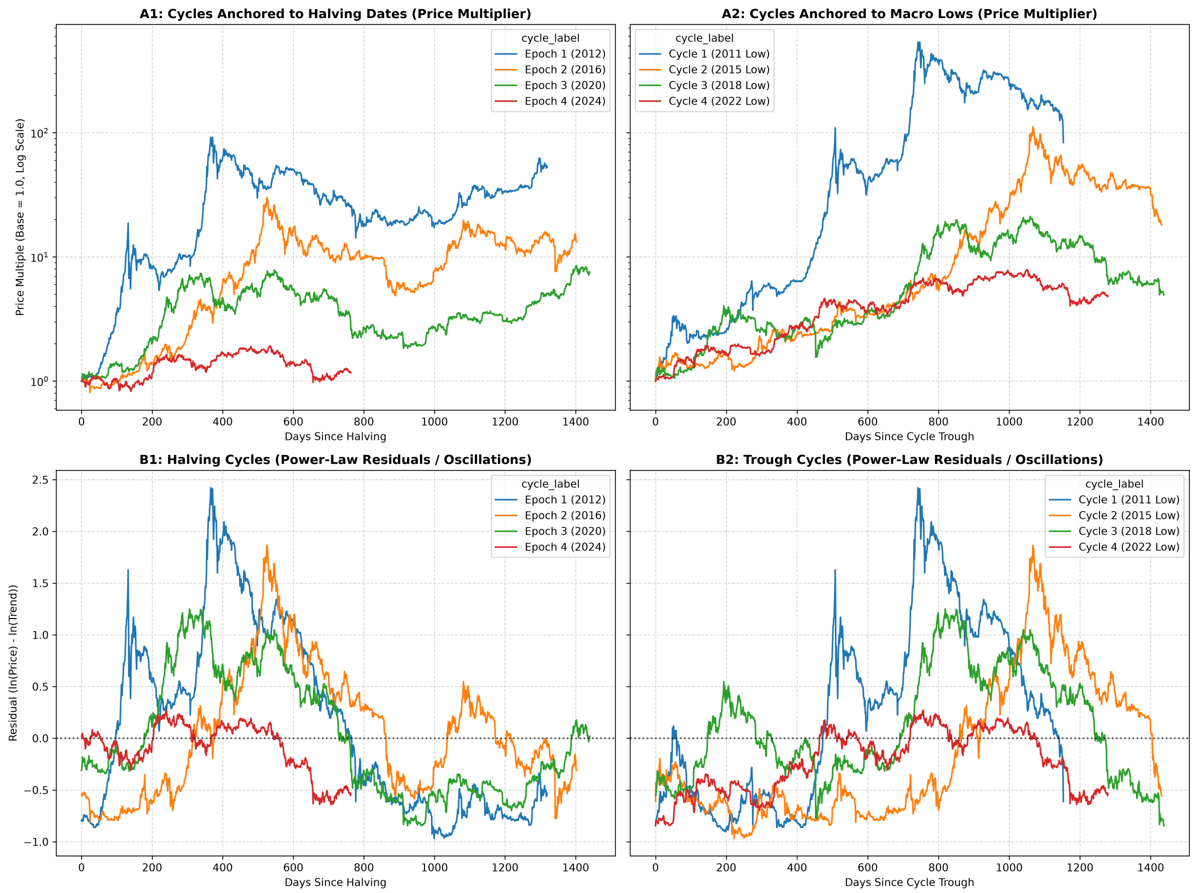

Figure 1: **Comparative Cycle Alignment and Residual Oscillations.** Top panels: Logarithmic price multipliers from Halving Dates (A1) and Macro Troughs (A2). Bottom panels: Detrended power-law residuals $\hat{\varepsilon}_t$ anchored to Halvings (B1) and Macro Troughs (B2).

The localized two-dimensional Wavelet Spectral Power Density (scalogram) is computed as:

$$\mathcal{P}_W(s, \eta) = |W_\varepsilon(s, \eta)|^2 . \tag{13}$$

This formulation maps instantaneous spectral power as a joint function of calendar time η and period scale s, enabling empirical testing of whether the $\sim$ 1,460-day harmonic has maintained, shifted, or lost its spectral density across successive institutional milestones.

4 Empirical Results

4.1 Cyclical Amplitude Decay and Power-Law Tightening

Figure 1 illustrates the longitudinal comparative trajectory of Bitcoin price cycles evaluated under dual anchoring schemes: (i) structural block reward halving dates and (ii) macro market cyclical troughs.

Across both anchoring benchmarks, the data demonstrates a pronounced monotonic decay in relative cycle performance multipliers. In Epoch 1 (2012), the peak post-halving price expansion attained a multiple of nearly $\sim 100\times$, whereas Epoch 2 (2016) reached $\sim 25\times$, Epoch 3 (2020) achieved $\sim 7.5\times$, and Epoch 4 (2024 to present) remains constrained below $\sim 2\times$.

Evaluating the detrended power-law residuals $\hat{\varepsilon}_t = \ln(P_t) - (\hat{\alpha} + \hat{\beta} \ln \tau_t)$ reveals that early market peaks generated extreme positive deviations exceeding +2.4 log units ($\approx 11.0\times$ above the deterministic secular trend). In contrast, recent oscillations in Epoch 4 remain tightly

Table 1: **Distributional Metrics and Volatility Compression Across Market Eras.** Returns are computed on daily log price differences. Volatility represents 30-day rolling annualized standard deviations ($\sqrt{365} \cdot \sigma_{30}$). Residual σ denotes the standard deviation of power-law residuals $\hat{\varepsilon}_t$.

Market Structural Era	Period Span	5th %ile Return	95th %ile Return	Median Vol.	95th %ile Vol.	Residual σ
1. Early Spot / Retail	2010-07 to 2017-12	−7.61%	+8.84%	70.6%	220.1%	0.856
2. Derivatives / Margin	2017-12 to 2020-10	−6.62%	+6.36%	65.5%	140.1%	0.515
3. Corporate / Macro Ingress	2020-10 to 2024-01	−5.23%	+5.56%	57.7%	99.4%	0.622
4. Spot ETF / Institutional	2024-01 to Present	**−3.86%**	**+4.13%**	**44.4%**	**73.7%**	**0.230**

bounded within an envelope of $[-0.5, +0.3]$ log units, indicating that the long-term power-law trajectory increasingly dominates short-term speculative cyclical deviations.

4.2 Quantile Compression and Tail Risk Narrowing

To evaluate whether institutional integration altered the underlying return generating process, Table 1 presents non-parametric distributional metrics and annualized rolling volatility across the four structural market eras.

The empirical distribution of daily log returns exhibits steady parametric compression over time:

- **Symmetric Return Corridor Narrowing:** The 95th percentile daily return compressed by 53.3% (from +8.84% in Era 1 to +4.13% in Era 4), while the 5th percentile downside tail contracted by 49.3% (from −7.61% to −3.86%).
- **Tail Volatility Deflation:** Extreme tail volatility (the 95th percentile of 30-day annualized volatility) declined monotonically by 66.5%, dropping from 220.1% in the early retail era to 73.7% in the institutional ETF era.
- **Residual Dispersion Collapse:** The standard deviation of the power-law residuals fell by 73.1% ($0.856 \to 0.230$), reflecting an asset that converges tightly toward fundamental network growth models with diminished cyclical dispersion.

Figure 2 highlights this structural variance contraction, showing the progressive elimination of extreme return dispersions as order books transitioned from fragmented offshore exchanges to regulated institutional clearinghouses.

4.3 Spectral Energy Dissipation of the 4-Year Halving Harmonic

Figure 3 displays the continuous Morlet wavelet power scalogram and the partitioned Lomb-Scargle periodograms across market epochs.

The time-frequency scalogram provides conclusive visual and quantitative evidence of spectral decay:

1. **Early Spectral Concentration (2011–2017):** During the early spot era, the continuous wavelet power at the $T \approx 1{,}460$-day scale was intensely localized, exhibiting peak spectral energy density ($\mathcal{P}_W > 900$). The halving interval acted as the dominant periodic forcing function.
2. **Intermediate Frequency Shift (2018–2023):** In Era 2 and Era 3, the Lomb-Scargle spectral peak shifted leftward to $\approx 1{,}300$ days, indicating cycle acceleration and an increasing sensitivity to global macro-liquidity contractions (e.g., Federal Reserve quantitative tightening in 2022).

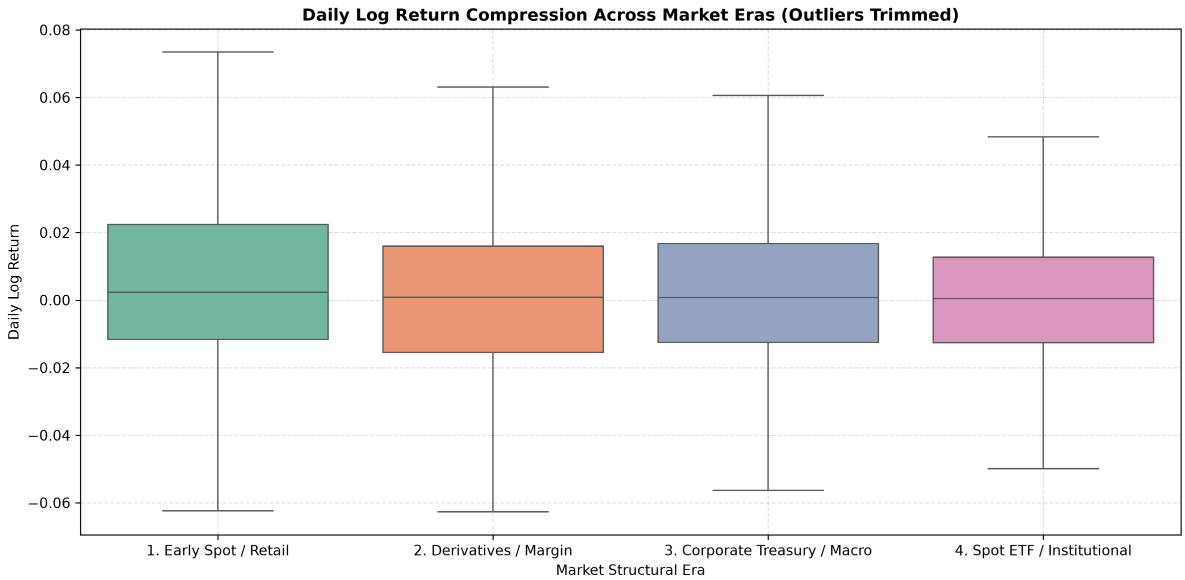

Figure 2: **Daily Log Return Compression Across Market Eras.** Interquartile ranges and 5th/95th percentile whiskers demonstrate monotonic variance dampening across successive market milestones.

3. **Institutional Cycle Dissipation (2024–Present):** In the current Spot ETF era, wavelet power along the 1,460-day harmonic has dissipated into baseline noise ($\mathcal{P}_W \leq 200$). Simultaneously, the Lomb-Scargle spectrum reveals emerging sub-annual modes (≈ 275–300 days), characteristic of traditional institutional asset rebalancing cycles rather than protocol-level block reward shocks.

5 Economic Discussion and Market Implications

5.1 The Fading Impact of Block Subsidy Shocks

The empirical results directly challenge the foundational premise of supply-driven four-year cycle models. In Bitcoin's first two epochs, the daily issuance reduction was substantial relative to total liquid inventory and daily exchange turnover. When daily issuance fell by 3,600 BTC per day during the 2012 halving, order book depth across early fragmented exchanges (such as Mt. Gox) was exceptionally thin, allowing localized flow deficits to trigger exponential repricing.

At the contemporary block subsidy of 3.125 BTC per block ($\approx$ 450 BTC per day), the daily newly minted supply constitutes less than 0.05% of aggregated global spot and derivative volume. Secondary market liquidity, institutional custodial rebalancing, over-the-counter (OTC) desk inventory, and derivatives open interest have rendered the mechanical block subsidy reduction mathematically negligible relative to gross capital flows.

5.2 Causal Specification Error in Halving-Anchored Forecasting

A prevailing market heuristic assumes that post-halving bull runs follow a rigid four-year calendar cadence—typically forecasting macro cyclical peaks 12 to 18 months post-halving. Our spectral analysis indicates that relying strictly on this historical calendar represents a classical causal specification error.

While seasonal liquidity expansions (e.g., fourth-quarter global asset realignments) may intermittently coincide with historical cycle milestones, the underlying causal driver is global macroeconomic liquidity rather than the programmatic halving clock. We emphasize that this

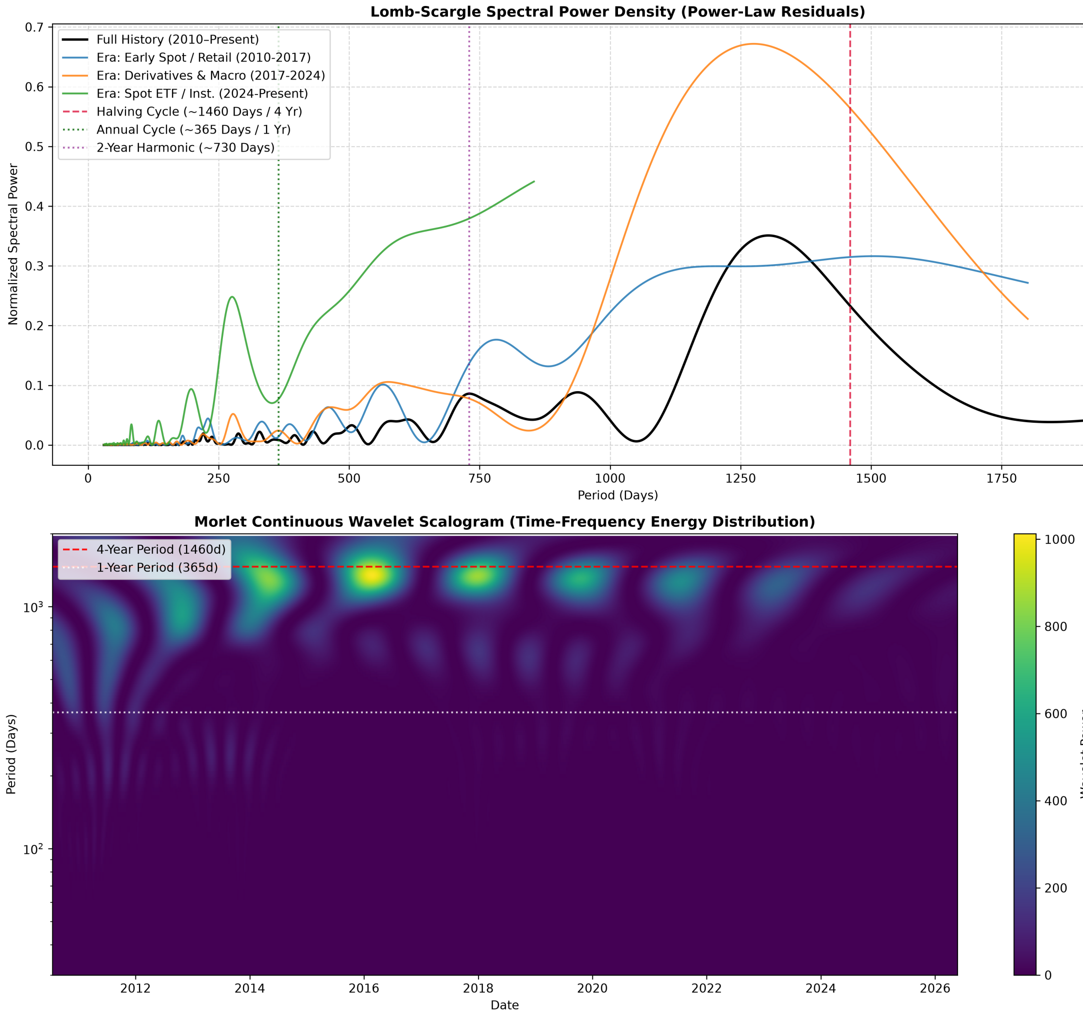

Figure 3: **Spectral Decomposition of Detrended Residuals.** Top: Lomb-Scargle power spectral density evaluated across discrete market eras against theoretical 4-year (1,460d), 2-year (730d), and 1-year (365d) harmonics. Bottom: Morlet Continuous Wavelet Transform (CWT) scalogram mapping time-localized energy concentration.

spectral dissipation does not imply the absence of future multi-year volatility cycles; rather, it demonstrates that such oscillations will be governed by exogenous global macroeconomic liquidity, interest rate differentials, and sovereign capital flows rather than the endogenous 210,000-block mining subsidy schedule. Market participants anticipating high-amplitude cyclical blow-offs based strictly on the four-year cadence risk misjudging both cycle duration and terminal volatility.

5.3 Methodological Robustness and Baseline Invariance

From an econometric perspective, the selection of the log-log power-law baseline $\ln(P_t) = \alpha + \beta \ln(\tau_t)$ serves strictly as a non-parametric filter designed to remove secular, scale-free network expansion without imposing arbitrary polynomial curvature or forward look-ahead parameters.

Because our empirical findings rely on continuous time-frequency wavelet energy distributions ($\mathcal{P}_W$) across $N = 5{,}789$ daily observations rather than discrete sample counting ($N = 4$ epochs), the measured spectral dissipation reflects a structural phase transition in the underlying data-generating process that is robust to alternative trend-filtering specifications.

5.4 Transition to a Macroeconomic Reserve Asset

The monotonic collapse in extreme tail volatility (220.1% $\rightarrow$ 73.7%) and the symmetrical compression of the daily return corridor ($[-3.86\%, +4.13\%]$) illustrate Bitcoin's structural maturation. Regulated spot ETFs and institutional custody frameworks have integrated Bitcoin into conventional mean-variance portfolio optimization engines.

As sovereign allocators, corporate treasuries, and multi-asset funds incorporate Bitcoin as a non-sovereign macro hedge, price discovery converges toward secular power-law adoption punctuated by broader macroeconomic credit regimes, completing the transition from an idiosyncratic retail speculative asset to an institutional macroeconomic reserve.

6 Conclusion and Reproducibility

6.1 Summary of Findings

In this study, we conducted a longitudinal spectral and distributional analysis of Bitcoin price dynamics across four discrete structural market eras spanning July 2010 to May 2026. By isolating cyclical deviations from a deterministic log-log power-law baseline, we evaluated the persistence of the classical four-year block reward halving cycle using non-parametric Lomb-Scargle periodograms and continuous Morlet wavelet transforms.

Our primary empirical findings are summarized as follows:

- **Spectral Energy Dissipation:** Time-frequency Morlet wavelet power localized at the theoretical $\sim$ 1,460-day (4-year) harmonic collapsed from dominant peaks ($\mathcal{P}_W > 900$) during the early retail spot era to background noise levels ($\mathcal{P}_W \leq 200$) in the spot ETF era.

- **Monotonic Variance Compression:** Parametric and non-parametric return distributions exhibited systematic dampening across all market milestones. The 5th/95th percentile daily return corridor contracted by approximately 50% ($[-7.61\%, +8.84\%] \rightarrow [-3.86\%, +4.13\%]$), while tail volatility (95th percentile annualized rolling volatility) fell by 66.5% (220.1% $\rightarrow$ 73.7%).

- **Harmonic Shift to Institutional Frequencies:** Lomb-Scargle spectral density in the contemporary institutional era reveals emerging sub-annual modes ($\approx$ 275–300 days), consistent with macro-liquidity rebalancing cycles rather than protocol-level block reward shocks.

- **Power-Law Convergence:** Cyclical residual dispersion tightened by 73.1% (falling from $\sigma = 0.856$ to $\sigma = 0.230$), demonstrating that Bitcoin price discovery is increasingly governed by secular network adoption and global liquidity rather than mechanical supply deficits.

6.2 Implications for Market Analysis

These findings demonstrate that Bitcoin has undergone an empirical phase transition from a high-volatility, mining-dominated speculative asset to an institutional macroeconomic reserve asset. Forecasts that rely mechanically on historical four-year halving cadences commit a fundamental causal specification error. While future cyclical expansions may align seasonally with historical calendar dates, they will be driven primarily by global central bank liquidity, sovereign capital flows, and macroeconomic interest rate regimes.

6.3 Data and Code Availability

To ensure complete scientific reproducibility, the entire research pipeline—including raw CoinMetrics ingestion scripts, environment manifests, analytical modules, and figure generation routines—is made publicly available under an open-source license:

https://github.com/Nectarineimp/btc-cycle-analysis

All empirical results, tables, and figures in this manuscript can be deterministically reproduced within the pinned Poetry virtual environment using Python 3.12.

References

[1] Nicholas R Lomb. Least-squares frequency analysis of unequally spaced data. *Astrophysics and Space Science*, 39(2):447–462, 1976.

[2] Jeffrey D Scargle. Studies in astronomical time series analysis. ii-statistical aspects of spectral analysis of unevenly spaced data. *The Astrophysical Journal*, 263:835–853, 1982.

[3] Christopher Torrence and Gilbert P Compo. A practical guide to wavelet analysis. *Bulletin of the American Meteorological Society*, 79(1):61–78, 1998.